

We are IntechOpen, the world's leading publisher of Open Access books Built by scientists, for scientists

6,900

Open access books available

186,000

International authors and editors

200M

Downloads

Our authors are among the

154

Countries delivered to

TOP 1%

most cited scientists

12.2%

Contributors from top 500 universities



WEB OF SCIENCE™

Selection of our books indexed in the Book Citation Index
in Web of Science™ Core Collection (BKCI)

Interested in publishing with us?
Contact book.department@intechopen.com

Numbers displayed above are based on latest data collected.
For more information visit www.intechopen.com



Dynamical Aspects of Apoptosis

Antonio Bensussen and José Díaz

*Theoretical and Computational Biology Group, Faculty of Science,
Autonomous University of Morelos, Cuernavaca, Morelos,
Mexico*

1. Introduction

Cells are dynamical systems characterized by a high degree of complexity due to an intricate network of subcellular processes that sustain their correct performance. This network is formed by a series of subnetworks with modular functioning, and among them is the subnetwork of biochemical processes that produces cell death or apoptosis. In this chapter we deal with the dynamical behavior of the apoptotic pathway activated by ionizing radiation (IR). In the special case of the apoptotic process, mathematical modeling is required for understanding its nonlinear complex behavior. Although previous attempts to model apoptosis were often limited to small systems, or based on qualitative data only, recent models are based on experimental data that give support to the theoretical results.

In this form, mathematical models have shown that the interactions between the nuclear molecular components of the intrinsic apoptotic pathway drive the system into a persistent limit cycle in the respective phase space after the application of high doses of ionizing radiation. Experimental data confirm the existence of this limit cycle, showing that this dynamical feature of the system relies on the existence of a p53-Mdm2 negative feedback loop, which is induced by a switch-like activation of the ATM kinase.

At the cytoplasm, the molecular dynamics that leads to the activation of the caspases sets up a saddle point bifurcation in the *caspase 3-Bax* degradation rate diagram. In this region of bistability, the saddle point bifurcation can drive the system either to a stable point with a high concentration of caspase 3 (cell death) or to a stable point with a low concentration of caspase 3 (cell survival). Out of this region, the system dynamics is settled on by the existence of a single stable fix point, which determines cell surviving independently of the concentration of caspase 3, i.e., there exists a threshold mechanism that regulates apoptosis and it is based on bistability, ultrasensitivity and irreversibility.

Thus, the main goal of this chapter is to review and analyze the recent knowledge about these nonlinear dynamical aspects of IR-induced apoptosis, in order to understand how this complex subnetwork of molecular interactions integrates the information coded in the signals that control the cell survival, and executes the corresponding action to determine the correct death-life decision. The modeling of such decisions has a significant impact on the field of radiation biology and in the therapeutic aspects of inducing apoptosis in cancer cells by IR.

2. Cell cycle and apoptosis

In recent decades cancer research has gained great importance worldwide, not only for being one of the most important chronic diseases of mankind, but also by the great

complexity of cellular process that it entails. A deeper insight into the causes of cancer progression, involves further research on the cell cycle because the malignant transformation starts as a deregulation of this cycle. In cancer, serious errors can be observed in DNA replication and repair simultaneously with an uncontrolled cell growth. Cancer cells lack the ability to respond to internal or external stimuli that induces death (Malumbres and Barbacid, 2009). It has been seen that between 50 and 70% of all cancer types are related to the absence of the transcriptional factor p53 (Vousden, 2006), which serves to activate the cellular repairing response to DNA damage.

2.1 Regulation of the cell cycle progression

The cell cycle has four phases. During the first phase (G1) the cell acquires the necessary nutrients for replication of the genetic material. If external signals are received, or the cell is ready to continue, then Cdc25 is activated (Budirahardja and Gönczy, 2009). Cdc25 activates Cdk4-cyclin-D and Cdk6-cyclin-D heterodimers (Malumbres, 2009). These heterodimers phosphorylate the Retinoblastoma protein (pRb) inducing the release of the E2F group of transcription factors (Abukhdeir and Park, 2009). These factors are necessary to transcribe genes that commit the cell to pass from G1 to S phase (Abukhdeir and Park, 2009) and to activate the first checkpoint, where is evaluated the genetic material integrity (Abukhdeir and Park, 2009). This test is performed by some specialized proteins such as ATM kinase (Ataxia-Telangiectasia Mutated), as well as some DNA binding proteins like the MRN complex (Pommier and Weinstein, 2006). If these proteins detect DNA damage, they induce cell cycle arrest through effector molecules such as Chk2, and p21Waf1/cip1 (Abukhdeir and Park, 2009). If the damage is severe, apoptosis is activated through the p53 pathway. If not damage in the DNA is detected; the cell induces degradation of cyclin D, activating the Cdk2-cyclin-E heterodimer, which is necessary to start the S phase (Malumbres and Barbacid, 2009).

The checkpoint commanded by ATM remains active during the S phase, in order to ensure the integrity of cell genome (Budirahardja and Gönczy, 2009). At the end of the S phase, the Cdk2-cyclin-A homodimer is activated to conclude the S phase, and the cell enters into G2 phase (Malumbres and Barbacid, 2009). After the cell has entered G2 phase, the activation of Cdk1-cyclin-B and Cdk1-cyclin-A heterodimers, in response to a mitogenic stimuli, starts M phase (Mitosis) (Pommier and Weinstein, 2006). It is noteworthy that the DNA damage sensors commanded by ATM are both active during transition from G2 to M and during the M phase (Calonge and O'Connell, 2008). After cytokinesis, cell can either enter to G1 phase or go out of cell cycle and remain in G0 state indefinitely (Calonge and O'Connell, 2008).

2.2 p53 network in stress-free conditions

The p53 transcription factor essentially serves to regulate the expression of genes responsible for the cell cycle arrest, repair of DNA damage, senescence and apoptosis in the intrinsic pathway (Lacroix et al., 2006). It is known that expression of the gene encoding p53 is dependent of the p50 subunit of NF- κ B transcription factor, and of other transcription factors like C/EPE β -2, Ets-1, Pitx1, p73 and p53 itself (Baillat et al., 2006; Wang et al., 2006; Boggs and Reisman, 2007; Wu and Lozano, 1994). In stress-free human fibroblasts, p53 interacts with the anti apoptotic BCL-XL protein in the cytoplasm, and forms a heterodimer (Dogu & Díaz, 2009), and the remaining fraction of p53 is marked in the carboxyl-terminus with a nuclear import signal (NLS1), and is subsequently transported to the nucleus, where

it will interact with the ubiquitin ligase Mdm2 (Hdm2 in humans). Mdm2 binds to p53, forming a complex that eventually will be degraded in the proteasome (Jänicke et al., 2008). It is noteworthy that at the basal level the Mdm2 gene promoter is activated by transcription factors other than p53, which have not yet been identified (Phelps et al., 2003). It is known that the *Mdm2* gene has two promoters (P1 and P2) that can lead to at least two isoforms of Mdm2 (Candeias et al., 2008). The p90Mdm2 isoform is responsible of the inhibition of *p53*, and the p76Mdm2 isoform is a p53 activator (Perry, 2004) and promotes the translation of p53 mRNA (Candeias et al., 2008). Under basal conditions p76Mdm2 expression is greater than p90Mdm2 (Phelps et al., 2004), and this fact could explain the origin of the basal levels of p53 throughout the cell cycle (Figure 1a). However, under cellular stress conditions, p53 induces the expression of p90Mdm2 in detriment of the p76Mdm2 isoform (Perry, 2004).

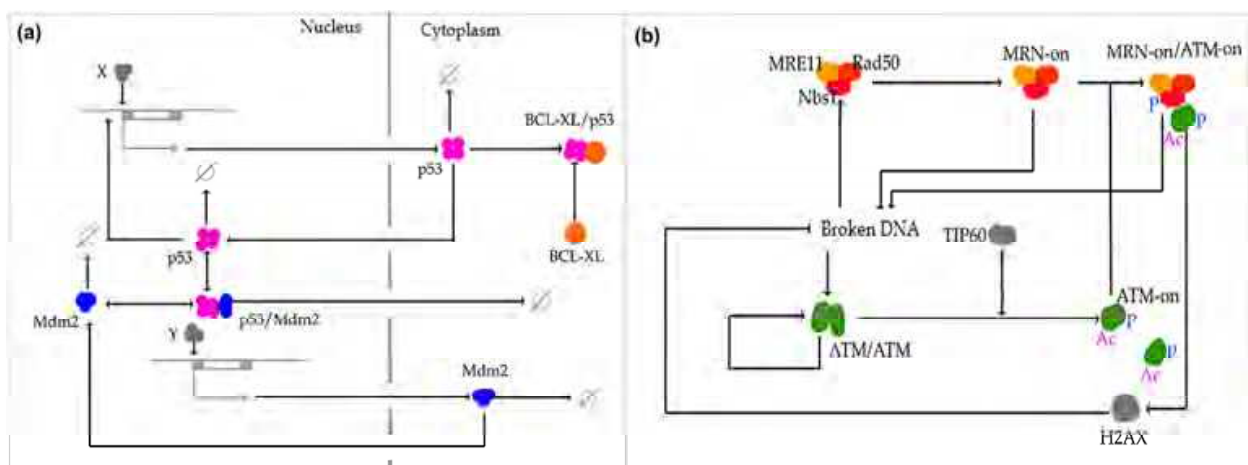


Fig. 1. (a) **p53 network at basal conditions.** p53 and other transcription factors, some of them no yet identified and marked as X, activates *p53* gene. Part of the novel p53 synthesized interacts with BCL-XL, forming heterodimers that will remain in the cytoplasm. The other part of p53 molecules is marked with an importation signal, enters the nucleus, and interacts with p90Mdm2 (represented by “Mdm2”) forming a complex that degraded in the proteasome. “Y” represents a transcription factor set that activates p90Mdm2 in absence of genotoxic stress, and the empty set symbol represents protein degradation. (b) **ATM activation network in response to DNA damage.** DNA damage causes a nuclear topology change that induces the self-phosphorylation of ATM homodimers (represented by ATM/ATM), allowing its separation into active monomers (represented by ATM-on). The ATM activation is full after that TIP60 acetylates it. In the other side, if MRN complex (forming by Mre11, Rad50 and Nds1) detects broken DNA, it will be activated (represented by MRN-on) and then it will bind to broken DNA, in order to stop the damage propagation. After ATM activation, it will phosphorylate various substrates including Nbs1, and this permits ATM union to MRN-broken DNA complex, in order to start the DNA damage repair signaling pathway, through activation of effector proteins like H2AX.

2.3 Cellular response to genotoxic stress, and its different scenarios

The cell is able to respond to genotoxic stress produced by various endogenous and exogenous agents like ionizing radiation (IR), viral infection, heat, growth factor deprivation and chemical DNA-damaging agents, among others (Plati et al., 2011). However, the mechanism and magnitude of the response will differ depending on both the

intensity and nature of the aggression. In particular, if the cell undergoes genotoxic stress there are three possible scenarios, and multiple combinations of them. The first scenario is when the cell suffers minor levels of DNA damage and can repair it successfully. The second scenario is when the cell suffers a medium damage in its DNA, and the cell has to “decide” between life and death. In this scenario it is possible that the cell die for not being able to fully repair the damage after a finite period of time, or live for being able to repair it. The third scenario is when the cell suffers severe damage, and initiates the apoptotic death. For a cell can be able of executing one of these three different responses, DNA damage intensity must be first detected, and then, the cell must “make the choice” of the appropriate scenario.

2.4 Detection of DNA damage

In genotoxic stress conditions, in response to DNA damage, the change in the nuclear topology, together with histone acetyl transferase Tip60, and the MRN complex (consisting of Mre11, Rad50, and Nbs1), induces the activation of ATM kinase (Sun et al., 2005; Vissers et al., 2008; Tanaka et al., 2007) (Figure 1b). After its activation, ATM phosphorylates histone H2AX and other proteins with a BRCT domain (such as Nbs1, 53BP1, and MDC1) for their activation (Vissers et al., 2008; Pommier and Weinstein, 2006). These proteins will bind to the broken DNA to stop the spread of damage (Vissers et al., 2008). Similarly, ATM activates Chk2 kinase, partially responsible for promoting cell cycle arrest, because it induces phosphorylation of Cdc25A and Cdc25C (Yoda et al., 2008; Pommier and Weinstein, 2006). Chk2 also promotes the activity of the transcription factor E2F-1 (Yoda et al., 2008), which, in turn, regulates Chk2 and ASPP protein expression (Bergamaschi et al., 2004).

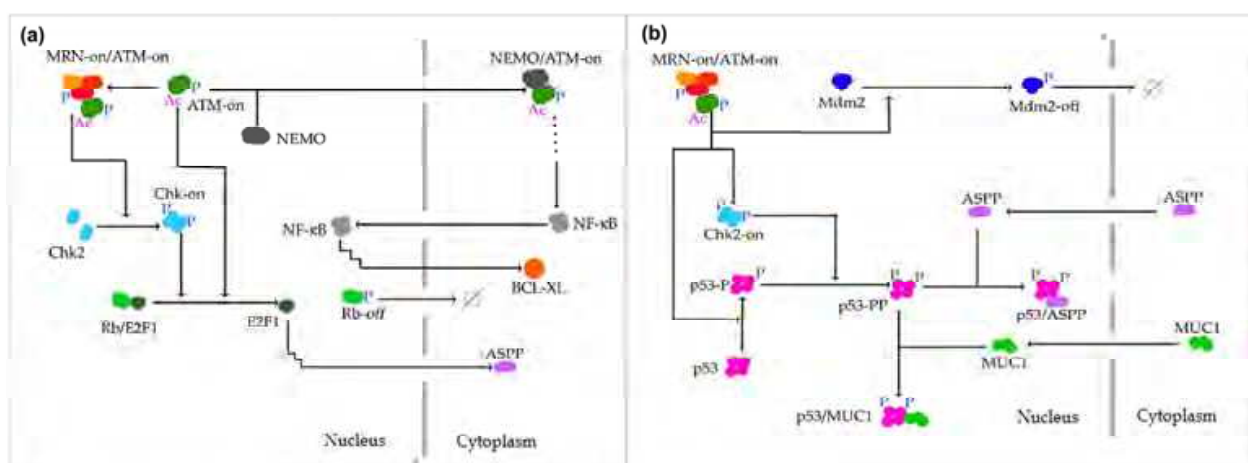


Fig. 2. (a) **Module of ATM effector functions.** When ATM is anchored to MRN-broken DNA complex, ATM phosphorylates Chk2 inactive monomers, to promote its binding into active homodimers. After that, free active ATM with Chk2 active homodimers will phosphorylate Rb protein to release E2F1. This transcription factor controls the pro-apoptotic protein synthesis, such as ASPP proteins. Free active ATM can bind to NEMO to induce NF-κB release in the cytoplasm. It is important because NF-κB is responsible to regulate the expression of proteins required to cell survival, like BCL-XL. In figure the stepped line represents the induction of protein transcription. (b) **The p53 activation by ATM and Chk2.** After the activation of ATM and Chk2, ATM inhibits Mdm2. Together with Chk2, ATM phosphorylates p53 in order to stabilize it. Phosphorylated p53 can bind either to MUC1 to promote the transcription of genes related with the cell cycle arrest and DNA damage repair, or can bind to ASPP proteins to promote the transcription of genes related with apoptosis.

In the nucleus, ATM interacts with NEMO forming a complex, which is ubiquitinated (Figure 2a), and transported to the cytoplasm where it induces the release of the transcription factor NF- κ B (Schmid and Birbach, 2008). After that, NF- κ B enters the nucleus and promotes the expression of various genes, including *BCL-XL* (Méndez et al., 2006; Chen et al., 2000). Simultaneously, ATM phosphorylates p53 nuclear stockpile, and, as a result, Mdm2 becomes less effective to recognize p53, delaying its degradation. Also, ATM phosphorylates Mdm2, inducing its autoubiquitination and degradation in the proteasome, and allowing an increase of p53 nuclear concentration over time (Dogu and Díaz, 2009). After ATM phosphorylation, Chk2 phosphorylates p53 in order to stabilize its structure (Pommier and Weinstein, 2006). At the end of this initial chain of phosphorylation, p53 can interact either with ASPP1 and ASPP2 proteins or with MUC1 (Pietsch et al., 2008). The MUC1 transmembrane glycoprotein is cleaved in response to a genotoxic stimuli and the cytoplasmic segment is targeted to the nucleus, allowing its union with phosphorylated p53 and the induction of cell arrest (Pietsch et al., 2008). On the other hand, in response to severe DNA damage (Figure 2b), p53 will bind mainly with ASPP proteins. The concentration of the ASPP proteins increases gradually due to the activity of E2F-1 (Pietsch et al., 2008; Braithwaite, 2006), enhancing the pro-apoptotic function of p53. In this form, depending on the intensity of the stimulus, p53 can be oriented to transcribe pro-apoptotic genes or anti-apoptotic genes, depending on the accessory proteins to which it is attached.

2.4.1 Irreversible DNA damage, death by apoptosis

When DNA damage signal is either too strong (Figure 3a), or persistent, and if the cell has no energy to repair damage, p53 binds to ASPP proteins, and interacts with the histone acetyltransferase p300/CBP to form a complex (Patel et al., 2008). After that, p300/CBP acetylates p53 on lysine 373, allowing the selective recognition of the promoter sites of pro-apoptotic genes like *PUMA*, *BAX* and *BAK* by p53 (Pietsch et al., 2008). It is noteworthy that the formation of the p53-p300 complex is reversible, and p300 is separated from the complex by the removal of the acetyl group of p53 (Pediconi et al., 2009). The enzyme responsible for this step is the SIRT1 deacetylase (Tanno et al., 2006; Pediconi et al., 2009). SIRT1 is an enzyme that uses NAD⁺ as cofactor from cellular metabolism. However, in this scenario of severe DNA damage, the effect of SIRT1 is negligible, but will be important in the third scenario discussed below.

2.4.2 Soft DNA damage, cell cycle arrest and successful repair of damage

When the DNA damage signal is weak (Figure 3b), MUC1 nuclear concentration increases, and the union between p53 and nuclear MUC1 is enhanced. After that, the complex p53-MUC1 interacts with PCAF (p300/CBP associated factor) to form a new complex (Pietsch et al., 2008). PCAF acetylates p53 on lysine 320, allowing it to specifically recognize the promoters of genes related with the cell cycle arrest like p21WAF1/cip1, and DNA damage repair (Pietsch et al., 2008). Similarly, SIRT1 opposes PCAF-dependent phosphorylation of p53, blocking its transcriptional activity when the cell does not have energy to express proteins (Yamamori et al., 2009; Pediconi et al., 2009; Ikenoue et al., 2008). However, SIRT1 is not the only control point of p53. As discussed above, ATM, along with NEMO, activates NF- κ B in its alternative pathway. This interaction is important, because NF- κ B promotes the expression of anti-apoptotic genes like *BCL-XL*. NF- κ B also competes with p53 for the cofactors: acetyltransferases p300, CBP and PCAF; which are required for the binding of p53

to DNA (Jänicke et al., 2008). The effect of this interaction leads to the indirect repression of the transcriptional activity of p53, given the fact that the concentration of the cofactors remains constant (Schmid and Birbach, 2008; Youle and Strasser, 2008).

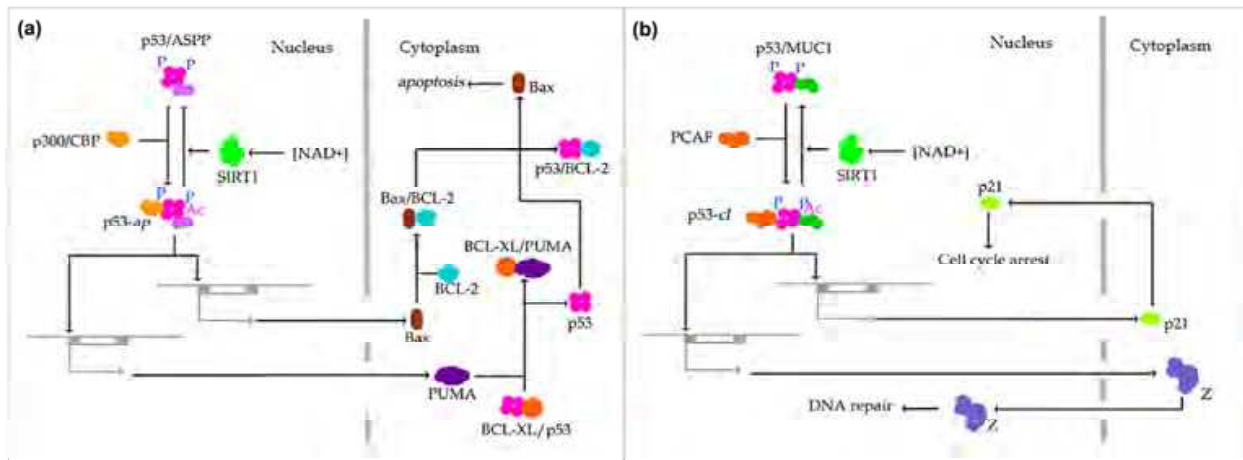


Fig. 3. (a) **The onset of apoptosis in its intrinsic pathway.** In response to severe DNA damage, p53 will bind to ASPP1 and ASPP2 (all of these are represented by ASPP). After that, p53-ASPP complex will interact with p300/CBP, and p300 acetylates p53-ASPP complex (represented by p53-ap). This allows p53-ap recognize the promoter side of apoptotic genes, like *PUMA* and *BAX*. The p53-ap transcriptional activity increases *PUMA* levels in the cytoplasm sufficiently to induce the release of p53 from p53/BCL-XL complexes. Free cytoplasmic p53 releases BAX in the cytoplasm starting C cytochrome-dependent apoptosis. (b) **Activation of cell cycle arrest and DNA damage repair pathways.** In response to medium intensity DNA damage, p53 will bind to MUC1. The p53-MUC1 complex interacts with PCAF (represented by p53-cl) to allow the expression of genes related with cell cycle arrest like *p21*, as well as the expression of genes related with DNA repair (in the figure are represented by "Z"). Another remarkable function of p53-cl is inducing the Wip1 and Mdm2 expression. Wip1 is a phosphatase that down-regulates the p53 network.

Among the p53-target genes that are activated in this pathway are WIP1 phosphatase and Mdm2 in its p90 isoform. The Wip1 function is to dephosphorylate Chk2, ATM, activated p53 and Mdm2 (Figure 4). This leads to inactivation of all of these proteins except Mdm2, which is activated (Braithwaite, 2006; Candeias et al., 2008; Kobet et al., 2000; Lahav et al., 2004; Jänicke et al., 2008; Bernards, 2004). The dephosphorylated form of Mdm2, activated WIP1, and new synthesized Mdm2, inhibit p53 reducing its nuclear concentration (Hu et al., 2007). Because the WIP1 function, the signal generated by ATM and Chk2 will blink while DNA damage is not repaired, since ATM activator proteins remain linked to broken DNA (Jänicke et al., 2008; Lu et al., 2008). When DNA damage is repaired nuclear topology is restored, and ATM activating proteins trigger stop signal. In this case, Wip1 definitely inactivates ATM, and effector molecules like Chk2. This encourages Mdm2 (p90 isoform) to efficiently suppress p53 activity (Figure 4). These interactions allow the cell to return to its basal state, and the levels of p90, Mdm2 and Wip1 also return to their basal value (Bernards, 2004).

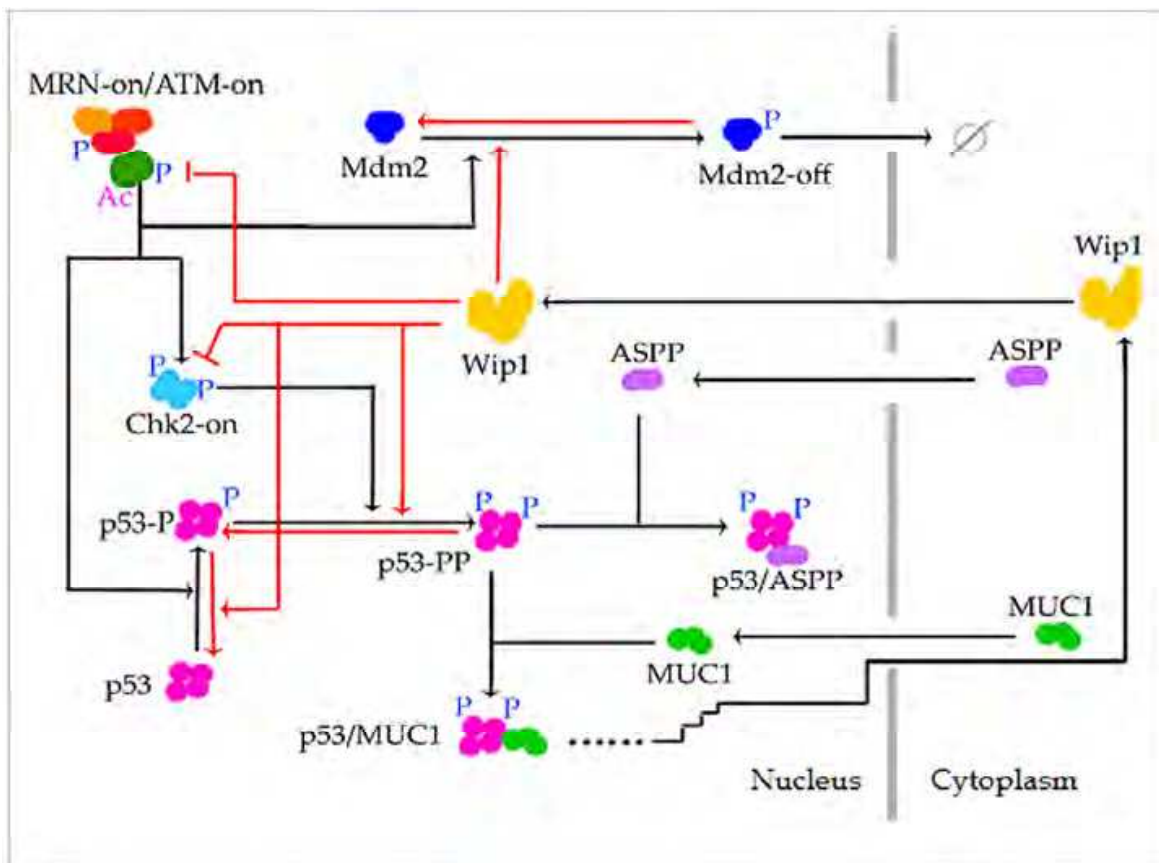


Fig. 4. **Mdm2 and Wip1 down-regulation of p53 network.** The main targets of Wip1 are ATM, Chk2 and Mdm2 phosphorylated. This results in a silencing of the ATM signal, and the Mdm2 activation. Mdm2 inhibits p53, in order to return its levels to normality, and restored the network equilibrium. In figure red lines represent the interactions that blocks Wip1.

2.4.3 Medium DNA damage, among life and death

The third stage is undoubtedly the most complicated of all, as it not only depends on the energy state of the cell, but also depends on the cell cycle phase in which the cell is. For example, if the cell is in S phase the cytoplasmic concentration of ASPP is higher than in other stages (Bermagaschi et al., 2004), and therefore this could lead more easily to apoptosis rather than cell cycle arrest. In this scenario, any type of delay suffered by the p53-dependent transcription process of the genes that control the DNA repair machinery and cell cycle arrest is of vital importance. These delays could be due to the effect of SIRT1 on p53, or to the competitive inhibition of p53 by other transcription factors, or to the action of the histone-acetyl transferases. If the transcription process of genes related to the DNA repair is slower than the normal, the cell will have fewer possibilities to survive. The intermittent signal of ATM produces a rise in the ASPP concentration, so it will be a question of time for the cell to enter in apoptosis. This could explain why after a long period of time if the cell is not repaired, it dies (Zhang et al., 2009; Yoda et al., 2001; Robinson et al., 2008; Shreeram et al., 2006; Wang et al., 2007; Bergamaschi et al., 2004; Braithwaite, 2006; Green and Kroemer, 2009; Toledo and Wahl, 2006; Liu et al., 2005; Haupt et al., 2006; Strano et al., 2006; Zhang et al., 2008).

3. Nonlinear cell dynamics

Cells are complex networks of physicochemical processes that support their highly organized structure and function. Thus, each cellular process sustained by a cell involves different levels of cellular organization. Each level of organization can be represented as a cell subsystem (subnetwork) that function in a modular mode (Thieffry and Romero, 1999; Del Vecchio, Ninfa and Sotang, 2008). In this form, cells can be modeled as formed by a set of subsystems like the regulatory genetic network, the network of synthesis and distribution of proteins, the network of signaling pathways, and the metabolic network, among others. The information flow through the set of cellular subsystems that controls the cell response to environmental signals occurs according to the canonical schema of Figure 5. Tumor-inducing DNA or RNA viruses, and other agents like ionizing radiation (IR), can drastically modify this flow of information.

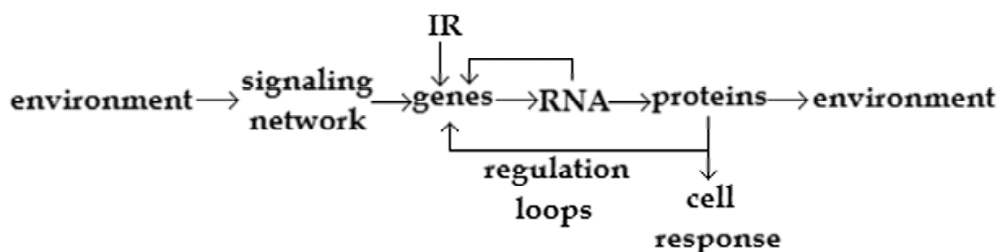


Fig. 5. **Flow of information between cell subsystems.** Changes in environmental conditions are sensed by cell signaling networks, which code and transmit this information to the nucleus. Coded information is decoded by the transcription machinery that, in response to this information, activates and inactivates a set of specific genes, giving raise to a specific distribution of effector proteins. These proteins are responsible for the cell specific response to the environmental conditions. Some of these proteins can be used to regulate gene expression, acting as specific transcription factors that conform complex regulatory loops inside the nucleus. Proteins can also be secreted to modify the cell environment. Tumor-inducing viral RNA and DNA can modify this flow of information by acting directly on the cell genome, drastically modifying the population of effector proteins and their function. Ionizing radiation (IR) can drastically interrupt this flow of information by producing severe damage to the cell DNA, and inducing apoptosis.

An important remark from Figure 5 is that the flow of information through cellular subsystems is due to a continuous flow of matter and energy, according to the respective laws of conservation. Taking into account the flow of matter at each point of the cell, the respective mass balance equation is:

$$\frac{\partial c_k(\mathbf{x}, t)}{\partial t} = \sum_r v_{rk} \cdot \omega_r(c_1(\mathbf{x}, t) c_2(\mathbf{x}, t) \dots c_k(\mathbf{x}, t) \dots c_s(\mathbf{x}, t)) + D_k \nabla^2 c_k(\mathbf{x}, t) \quad (1)$$

which means that the local rate of variation of the concentration of the substance k (denoted by c_k) at point \mathbf{x} at time t is equal to the net rate of diffusion of k inside the cell volume V (denoted by $D_k \nabla^2 c_k(\mathbf{x}, t)$) plus the rate of formation/degradation of k due to the local chemical reactions inside V . In equation (3.1), ω_r represents the local rate of the chemical reaction r , which is a functional of the concentration of the reactive substances at point \mathbf{x} at time t , and v_{rk} is the stoichiometric coefficient of k in reaction r .

The reaction term of equation (1) can be rewritten as:

$$\sum_r \nu_{rk} \cdot \omega_r (c_1(\mathbf{x}, t) c_2(\mathbf{x}, t) \dots c_k(\mathbf{x}, t) \dots c_s(\mathbf{x}, t)) = f_k(c_1(\mathbf{x}, t), c_2(\mathbf{x}, t), \dots, c_k(\mathbf{x}, t), \dots, c_s(\mathbf{x}, t)) \quad (2)$$

$$k = 1, 2, \dots, s$$

leading to:

$$\frac{\partial c_k(\mathbf{x}, t)}{\partial t} = f_k(c_1(\mathbf{x}, t), c_2(\mathbf{x}, t), \dots, c_k(\mathbf{x}, t), \dots, c_s(\mathbf{x}, t)) + D_k \nabla^2 c_k(\mathbf{x}, t) \quad k = 1, 2, \dots, s \quad (3)$$

which is the well known form of the reaction-diffusion equation for the substance k . It indicates that the temporal variation of the concentration of k at point \mathbf{x} at time t depends on the balance between the chemical processes in which this substance takes part, represented by the function f_k , and its diffusion rate in the cellular medium. Function f_k is generally a nonlinear function of the concentration of the reactive substances, and equation (3) usually has not an analytical solution. In a homogeneous medium the diffusive term in equation (3) is null, and f_k completely defines the entire system dynamics in the s -dimensional phase space, which is defined by the set of concentration values of the s reactive substances. The systems dynamics is represented by a trajectory in this space, defined by the column vector $\mathbf{c}(t) = \langle c_1(t) c_2(t) \dots c_s(t) \rangle$. In nonlinear systems this trajectory can have peculiar characteristics like high sensitivity to initial conditions, bifurcations and complex loops that represent a great variety of dynamical behaviors observed in biological systems like limit cycles, hysteresis, bistability, ultrasensitivity, among others. In not homogeneous medium the diffusive term of equation (3) produces a more complex dynamical behavior of the system, giving rise to phenomena like traveling waves, spirals and spatially located bursting of second messengers and proteins, among others.

In the subsequent sections it is discussed in depth the nonlinear dynamics of homogenous chemical systems.

3.1 Stability of nonlinear systems

The first problem concerning the dynamics of nonlinear systems is the determination the steady points of the system in its phase space.

A steady point is a column vector $\mathbf{c}^o = \langle c_1^o(t) c_2^o(t) \dots c_s^o(t) \rangle$ for which equation:

$$\dot{\mathbf{c}}(t) = \mathbf{f}(\mathbf{c}(t)), \text{ where } \mathbf{f}(\mathbf{c}(t)) = \begin{bmatrix} f_1(c_1(t), c_2(t), \dots, c_k(t), \dots, c_s(t)) \\ \vdots \\ f_s(c_1(t), c_2(t), \dots, c_k(t), \dots, c_s(t)) \end{bmatrix} \quad (4)$$

becomes zero. Once the set of steady points of the system is settled on, is necessary to determine their stability. Equation (4) subject to the initial condition $\mathbf{c}(0) = \mathbf{c}_0$ defines a **nonlinear dynamical system**.

The steady point \mathbf{c}^o of a dynamical system is **Liapunov stable** if for each $\varepsilon > 0$ exists a $\delta > 0$ such that $\|\mathbf{c}(t) - \mathbf{c}^o\| < \varepsilon$ whenever $\|\mathbf{c}(0) - \mathbf{c}^o\| < \delta$, i.e., any trajectory that initiates at a distance δ of the steady point \mathbf{c}^o remains at a distance ε of it for all positive time.

The steady point \mathbf{c}^o of a dynamical system is attracting if exists a $\delta > 0$ such that $\lim_{t \rightarrow \infty} \mathbf{c}(t) = \mathbf{c}^o$ for any trajectory $\mathbf{c} = \mathbf{c}(t)$ whenever $\|\mathbf{c}(0) - \mathbf{c}^o\| < \delta$, i.e., any trajectory that initiates at a distance δ of the steady point \mathbf{c}^o will converge to it eventually. In this case, the point \mathbf{c}^o is an **attractor** of the dynamical system in the phase space. A steady point \mathbf{c}^o , which is Liapunov stable and attracting, is asymptotically stable.

A steady point \mathbf{c}^o , which is neither stable nor attracting, is unstable and is a **repulsor** in the phase space.

3.2 Phase plane analysis

In nonlinear systems the trajectories cannot be generally determined in an analytical form. However, it is possible to perform a qualitative analysis to find out the global behavior of the dynamical system in the corresponding phase space. As a vector can be assigned to each point of this space, according to equation (4), the vector field associated to the phase space can be drawn. By flowing this vector field, a phase point traces a solution $\mathbf{c}(t)$ of the dynamical system, corresponding to a trajectory winding through the phase space.

It is of importance to point out the fact that if the function \mathbf{f} of equation (4) is continuous and all its partial derivatives $\frac{\partial f_i}{\partial c_j}$ $i, j = 1, 2, \dots, s$ are also continuous in \mathbf{c} for a given subset

$D \subset \mathfrak{R}^n$, then for every $\mathbf{c}_0 \in D$ the initial value problem of equation (4), has solution $\mathbf{c}(t)$ in some time interval $(-t, t)$ around $t = 0$ and this solution is unique. A topological implication of this theorem is that two trajectories cannot intersect and, as consequence, chaos is ruled out of any 2-dimensional phase space but arises as a possible behavior of every s -dimensional dynamical system with $s > 2$ (Strogatz, 1994).

The phase space analysis of the dynamics of a nonlinear system takes into account the following aspects: 1) the number, position and stability of the steady points; 2) the arrangement of the trajectories near the steady points; and 3) the existence and stability of closed orbits.

In section 3.1 was presented the form in which the steady points are determined and how they can be classified according to their stability. The arrangement of the trajectories around steady points is determined by linearization of the original nonlinear system, and analysis of the behavior of the eigenvalues of the Jacobian matrix of the linearized system around each steady point. For example, considering a 2-dimensional phase space and a steady point $\mathbf{c}^o = \langle c_1^o, c_2^o \rangle$, a small perturbation from this steady state drives the nonlinear dynamical

system $\begin{bmatrix} \dot{c}_1(t) \\ \dot{c}_2(t) \end{bmatrix} = \begin{bmatrix} f_1(c_1(t), c_2(t)) \\ f_2(c_1(t), c_2(t)) \end{bmatrix}$ into a new trajectory $\delta \mathbf{c}(t) = \langle \delta c_1(t), \delta c_2(t) \rangle$,

where $\delta c_1(t) = c_1(t) - c_1^o$ and $\delta c_2(t) = c_2(t) - c_2^o$. In this form:

$$\begin{aligned} \delta \dot{c}_1 = \dot{c}_1 &= f_1(c_1^o, c_2^o) + \left. \frac{\partial f_1}{\partial c_1} \right|_{(c_1^o, c_2^o)} \delta c_1 + \left. \frac{\partial f_1}{\partial c_2} \right|_{(c_1^o, c_2^o)} \delta c_2 + O(\delta^2 c_1, \delta^2 c_2, \delta c_1 \delta c_2) \\ &= \left. \frac{\partial f_1}{\partial c_1} \right|_{(c_1^o, c_2^o)} \delta c_1 + \left. \frac{\partial f_1}{\partial c_2} \right|_{(c_1^o, c_2^o)} \delta c_2 + O(\delta^2 c_1, \delta^2 c_2, \delta c_1 \delta c_2) \quad \text{because } f_1(c_1^o, c_2^o) = 0 \end{aligned} \quad (5)$$

in a similar form:

$$\delta \dot{c}_2 = \dot{c}_2 = \frac{\partial f_2}{\partial c_1} \bigg|_{(c_1^o, c_2^o)} \delta c_1 + \frac{\partial f_2}{\partial c_2} \bigg|_{(c_1^o, c_2^o)} \delta c_2 + O(\delta^2 c_1, \delta^2 c_2, \delta c_1 \delta c_2) \quad (6)$$

which leads to the linearized dynamical system:

$$\begin{bmatrix} \delta \dot{c}_1(t) \\ \delta \dot{c}_2(t) \end{bmatrix} = \begin{bmatrix} \frac{\partial f_1}{\partial c_1} \bigg|_{(c_1^o, c_2^o)} & \frac{\partial f_1}{\partial c_2} \bigg|_{(c_1^o, c_2^o)} \\ \frac{\partial f_2}{\partial c_1} \bigg|_{(c_1^o, c_2^o)} & \frac{\partial f_2}{\partial c_2} \bigg|_{(c_1^o, c_2^o)} \end{bmatrix} \begin{bmatrix} c_1(t) \\ c_2(t) \end{bmatrix} = \mathbf{J}[c_1, c_2] \begin{bmatrix} c_1(t) \\ c_2(t) \end{bmatrix} \quad (7)$$

$\mathbf{J}[c_1, c_2]$ represents the Jacobian matrix of the linearized dynamical system in equation 6. The eigenvalues λ_1, λ_2 of $\mathbf{J}[c_1, c_2]$ can be calculated from the characteristic equation: $|\mathbf{J}[c_1, c_2] - \lambda \mathbf{I}| = 0$. Depending on the nature of the eigenvalues, it is possible to know the arrangement of the trajectories near each steady point of the nonlinear system (Figure 6). This linearization process can be extended to perform the phase space analysis of higher dimensional nonlinear dynamical systems (Edelstein-Kesher, 2005).

An important question that arises at this point is whether the behavior of the trajectories obtained from equation (7) accurately reflects the real behavior of the trajectories of the original nonlinear system. Andronov et al. (1973) show that this is the case. If the linearized system has a saddle, a node or a spiral at a given steady point, then the original nonlinear system really has also a saddle, a node or a spiral at that steady point. Furthermore, if a steady point is a stable saddle or node of the linearized dynamical system, then it is also a stable saddle or node of the nonlinear system. In this case, the neglected nonlinear terms of equations (5) and (6) practically have no effect on the stability of these points when $\text{Re}(\lambda) \neq 0$ for both eigenvalues. This kind of steady points is known as **hyperbolic points**, and they are not affected by the small nonlinear perturbations. The topological implication of this fact is that the vector field corresponding to a saddle or a node is not altered by small nonlinear perturbations and, as consequence, has **structural stability** (Strogatz, 1994).

When the eigenvalues of the Jacobian matrix are pure imaginary $\lambda = \pm i$, the steady point is a center. The trajectories around this point are closed orbits that are stable. However, the neglected nonlinear terms in equations (5) and (6) can produce an imperfect closure of the orbit, giving rise to a spiral. In this form, the vector field corresponding to a center is altered by small nonlinear perturbations that transform the center into a spiral and, as consequence, has no structural stability (Strogatz, 1994).

According to their stability, steady points of 2-dimensional dynamical systems can be classified into a: 1) **Robust case**, which includes repellers or sources, for which both eigenvalues have $\text{Re}(\lambda) > 0$; attractors or sinks, for which both eigenvalues have $\text{Re}(\lambda) < 0$ and saddles, for which one eigenvalue has $\text{Re}(\lambda) > 0$ and the other one has $\text{Re}(\lambda) < 0$; 2) **Marginal case**, which includes centers for which both eigenvalues are pure imaginary, and non-isolated steady points for which one eigenvalue has $\text{Re}(\lambda) = 0$ (Strogatz, 1994).

However, the phase space of a nonlinear system can exhibit another kind of closed orbits called **limit cycles**, which cannot be observed in linear systems. A limit cycle is an isolated

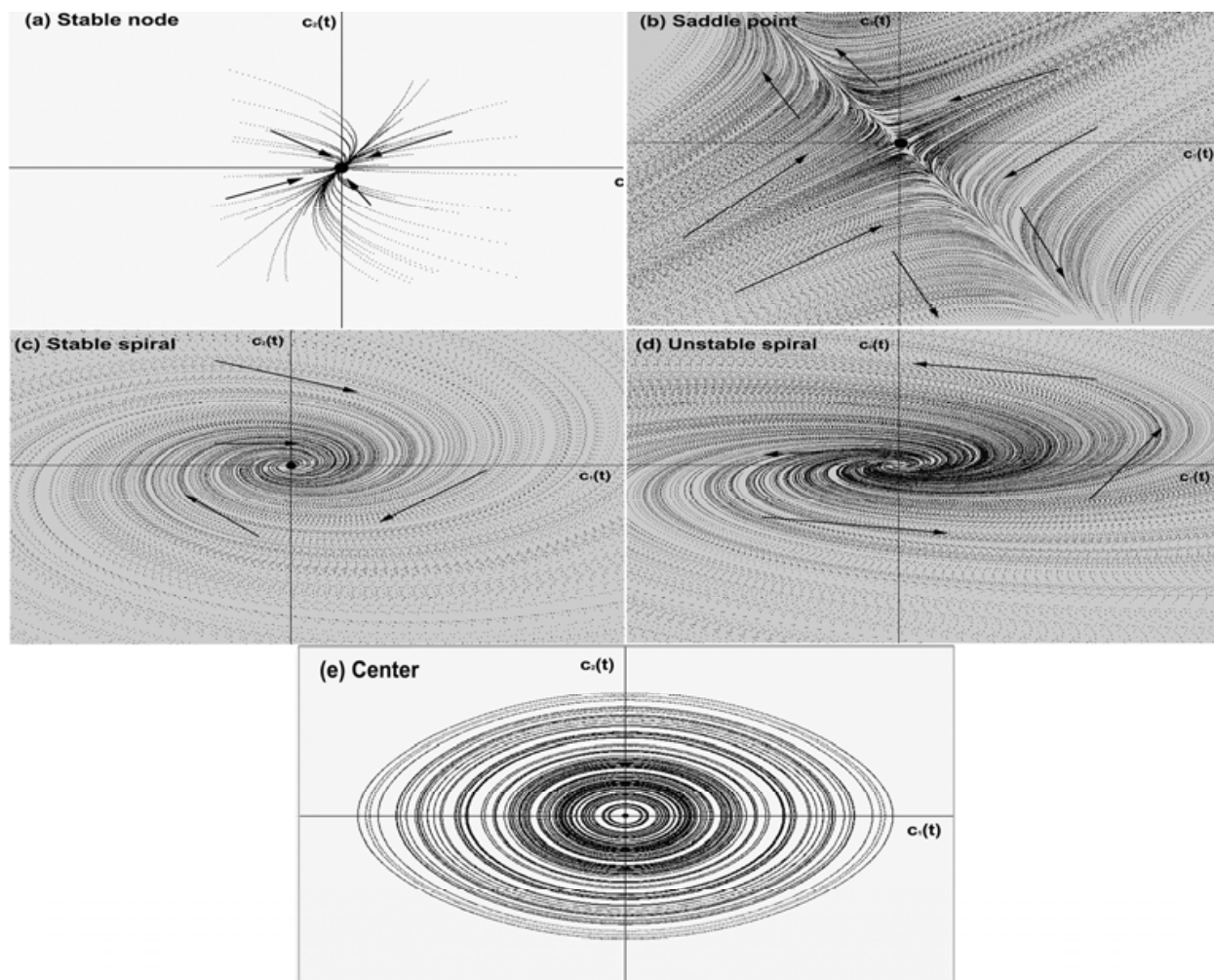


Fig. 6. Classification of the steady points of a 2-dimensional linearized dynamical system.

(a) There is a stable node or attractor in the phase space when both eigenvalues λ_1 and λ_2 are real and negative (when both eigenvalues are positive, the steady point is a unstable node or repulsor); (b) There is a saddle point in the phase space when both eigenvalues λ_1 and λ_2 are real, but one of them is positive and the other is negative. The stable manifold is spanned by the eigenvector associated to the negative eigenvalue. The unstable manifold is spanned by the eigenvector associated to the positive eigenvalue. (c) There is a stable spiral in the phase space when both eigenvalues λ_1 and λ_2 are complex conjugated with negative real part. (d) On the contrary, if both eigenvalues λ_1 and λ_2 are complex conjugated with positive real part the spiral is unstable. (e) When λ_1 and λ_2 are pure imaginary the steady point is a center surrounded by a series of stable closed orbits. All figures show the flow of the dynamical system in the phase space spanned by the basis conformed by the variables $c_1(t)$ and $c_2(t)$. The black point represents the steady point of the dynamical system, and the arrows mark out the direction of the flow of the vector field.

trajectory for which neighbor trajectories can be only spirals that converge to it or diverge from it. If all the spirals converge into the limit cycle, this closed orbit is stable, otherwise is unstable. The existence of this kind of closed trajectories in the plane is settled down by the Poincaré-Bendixson theorem. According to this theorem, exists a trajectory C , which is either a closed orbit or a spiral that converges to a closed orbit as $t \rightarrow \infty$, confined inside a certain closed bounded region R of the plane. This theorem assumes 1) the existence of a vector

field $\dot{\mathbf{c}} = \mathbf{f}(\mathbf{c})$ that is continuously differentiable on an open set of the plane containing R and 2) R does not contain any fixed point (Edelstein-Keshner, 2005). A consequence of this theorem is that in a 2-dimensional phase space any trajectory trapped into a closed bounded region R must converge to a limit cycle.

However, in higher dimensional systems the Poincaré-Bendixon theorem does not longer apply and trajectories can be trapped into a closed region of the phase space without converge into a limit cycle or settle down to a fixed point, and they could be attracted by a complex geometric object called strange attractor, which is a fractal set on which the motion is aperiodic and sensitive to very small changes in initial conditions. This sensitivity makes the motion unpredictable as t increases, giving rise to a chaotic dynamics (Strogatz, 1994).

3.3 Bifurcations

The qualitative features of the vector field of a biochemical dynamical system are strongly dependent on the set of parameters of its corresponding set of differential equations. As the value of one of these parameters changes, the qualitative features of the vector field undergo local variations around the steady points. This parameter-dependent change in the local topological structure of a vector field is known as bifurcation. They generally occur in a one-dimensional subspace, and the rest of the dimensions of the phase space are affected as consequence of the flow that can be attracted or repelled from this subspace (Strogatz, 1994; Edelstein-Keshner, 2005). Taking into consideration the imaginary plane, we can roughly classify bifurcations into two cases: 1) the eigenvalues of the Jacobian matrix are both real and bifurcations occur along the real axis as certain parameter α changes. This kind of bifurcation comprises the saddle-node bifurcation; the transcritical bifurcation, and the subcritical and supercritical pitchfork bifurcation. 2) The eigenvalues of the Jacobian matrix are complex conjugated. Bifurcations occur crossing the imaginary axis as certain parameter α changes. This kind of bifurcation comprises the supercritical and subcritical Hopf bifurcation.

In the first case, a) the saddle-node bifurcation causes local variations in the vector field around two points: a saddle and a node, as a bifurcation parameter α changes. These points become closer as parameter α varies until they collide and annihilate each other. This type of bifurcation has interesting applications in some models of biological processes that imply the presence of chemical switches; b) a transcritical bifurcation occurs when two steady points interchange their stability as the bifurcation parameter α varies. c) The normal form of an ordinary differential equation (ODE) that exhibits a subcritical pitchfork bifurcation is $\dot{c} = \alpha c + c^3$. When $\alpha < 0$ the steady point $c = 0$ is stable and there are two unstable points at $c = \pm\sqrt{-\alpha}$. When $\alpha > 0$ the only real steady point $c = 0$ becomes unstable. The normal form of an ODE that exhibits a supercritical pitchfork bifurcation is $\dot{c} = \alpha c - c^3$. When $\alpha < 0$ the only real steady point $c = 0$ is stable. For $\alpha > 0$ there is an unstable steady point at $c = 0$ and to stable steady points at $c = \pm\sqrt{\alpha}$.

In the second case, the presence of a Hopf bifurcation leads the system to a limit cycle. As the bifurcation parameter α varies, when a certain critical value α_c is reached the supercritical Hopf bifurcation drives the transformation of a stable spiral into an unstable spiral that converges to a stable limit cycle (Figure 7). The case of a subcritical Hopf bifurcation is more complicated. A typical example is when an unstable limit cycle shrinks to zero amplitude as the bifurcation parameter α reaches its critical value α_c , at which the

cycle engulfs the node rendering it unstable and making the system to jump to a distant attractor when $\alpha > \alpha_c$ (Strogatz, 1994; Edelstein-Keshner, 2005). This new attractor could be a steady point, another limit cycle, infinity or a chaotic attractor (for higher dimensional systems).

4. Dynamical aspects of apoptosis

Ionizing radiation is a term applied to radiation that has energy enough to remove an electron from an atom or molecule. This ionization can produce free radicals chemically reactive. The effect of the ionizing radiation depends only on the energy of the particles (photons, electrons or α particles) that impacts a particular target. The effect of the ionizing radiation is measured in gray (Gy), which is the SI unit of **absorbed dose**, and is equivalent to the amount of radiation necessary to deposit one Joule of energy in one kilogram of matter. Ionizing radiation is used in the treatment of various types of cancer, under the assumption that the apoptotic network of cancer cells is disabled, making these cells more susceptible to the effects of single and double strand damage in their DNA (Qi et al., 2007).

4.1 Oscillatory nuclear dynamics of p53 in response to ionizing radiation

The response of a nonlinear dynamical system to an input is **digital**, when the output is conformed by a series of periodic discrete pulses or quanta, that have fixed form and size. The number of pulses increases with the strength of the input signal. The digital response corresponds to a limit cycle, which is generally driven by the onset of a **supercritical Hopf bifurcation** (Ma et al., 2005; see section 3.3 and Figure 7). In contrast, the response to a given input is **analog** when the strength of the output increases with the strength of the input signal (Lahav et al., 2004). Recent results show that the kind of radiation applied to a cell can produce different dynamical effects, either digital or analog, depending on the molecular subnetwork activated in response to the **double strand breaks** (DSB's) produced (Batchelor et al., 2011).

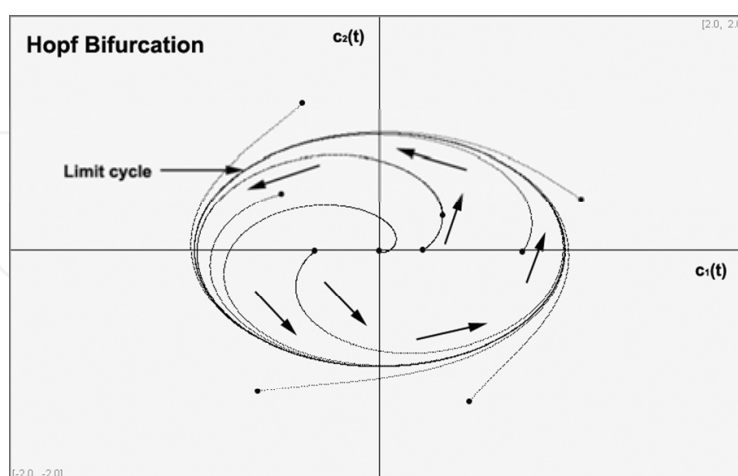


Fig. 7. **Supercritical Hopf bifurcation.** This kind of bifurcation transforms a stable spiral into an unstable spiral that converges to a stable limit cycle when the value of the bifurcation parameter α reaches some critical value α_c . The black points in the figure are different initial conditions of the dynamical system. The arrows mark out the direction of the flow of the vector field. The phase space is spanned by $c_1(t)$ and $c_2(t)$.

When γ -radiation or the radiomimetic drug neocarzinotastina (NCS) are applied to a cell, the output is digital. According to the results of Batchelor et al. (2008, 2011), the DSB's produced by these agents induce the onset of a limit cycle of fixed duration, amplitude and period (~ 5 h) in the p53-Mdm2 phase space. The number of pulses of both molecules increases as the damage increases. This series of pulses have the characteristic of an "all or none" response in single cells, which is triggered even by transient inputs (Batchelor et al., 2008).

A previous model by Ma et al. (2005) predicts this kind of digital dynamics under two basic facts: 1) the number of DSB's for a given doses is stochastic and follows a Poisson distribution with an average proportional to the radiation dose applied x and given by $35x$, which is consistent with the observed 30-40 DSB's per Gy. The repair dynamics is simulated with a Monte Carlo method; 2) the repairing of the DNA damage is a biphasic process, i.e., consists of a rapid and a slow phases of DSB fix, which are assumed to be produced by two different types of DSB's. The simple DSB's, which contain a break in each strand of DNA of a short segment of 10-20 bps in length, switches on the fast repairing process. The slow repairing process is triggered by complex DSB's, which contains breaks in each strand of DNA, together with other kind of alterations like base damage, base deletions, etc., within the same short segment. The fast and slow processes are represented by different chemical kinetics (Stewart, 2001).

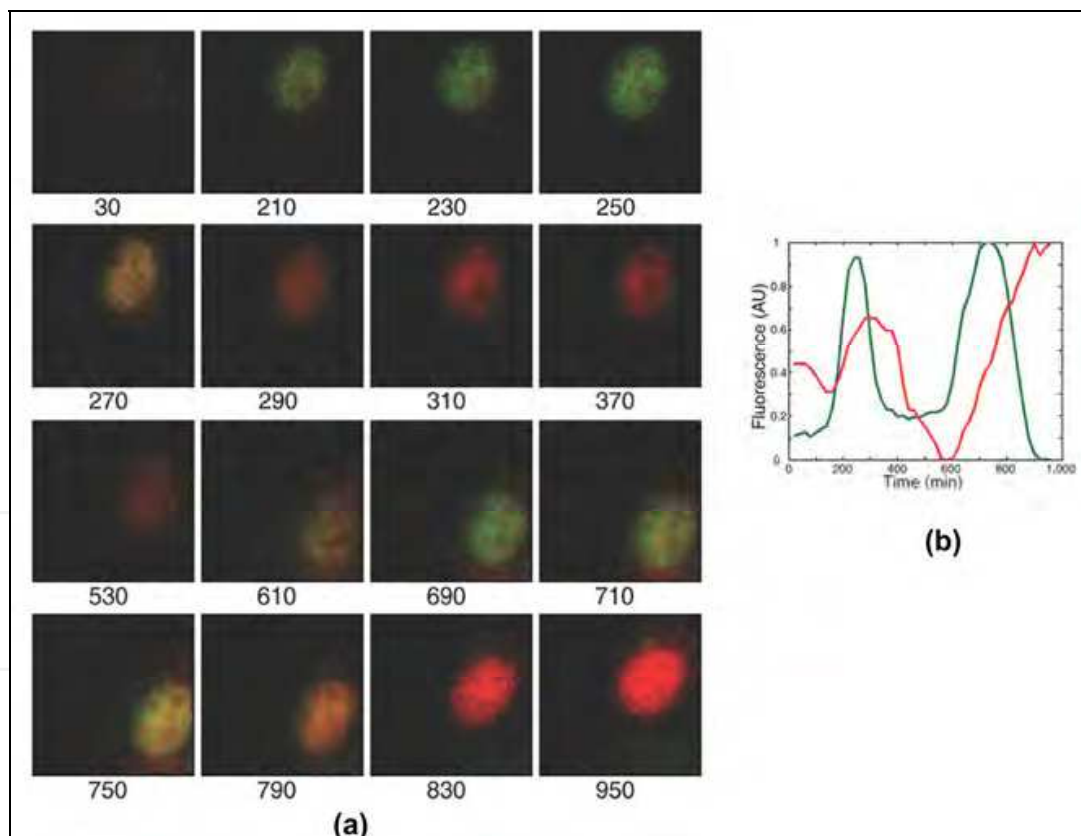


Fig. 8. (a) **Experiments with fluorescent p53 and Mdm2.** Two pulses of p53-CFP (green) and Mdm2-YFP (red) are shown in this panel. Time (in min) after irradiation is show below images. In the figure, a phase difference of ~ 120 min between the p53 and Mdm2 maximum fluorescence is observed. (b) **Levels of p53-CFP and Mdm2-YCP in the nucleus** of the cell of panel (a). AU, arbitrary units. Figure reproduced from Lahav et al. (2004), with authorization of Dr. U. Alon.

As mentioned above, the predicted dynamics from this model is a digital output, in which doses of the order of 5 Gy (~ 150 DSB's) applied in an on - off form produces pulses of p53 and Mdm2 with a period of ~ 7 hr and a phase difference of ~ 115 min. These results are consistent with the experimental results of Lahav et al. (2004) that are showed in Figure 8.

In order to study the behavior of the p53 and Mdm2 loop in individual MCF7 breast cancer cells, Lahav et al. (2004) fused p53 with the cyan fluorescent protein (CFP) under a zinc-inducible promoter, and Mdm2 with a yellow fluorescent protein (YFP) under the human Mdm2 native promoter. p53-CFP was completely functional in induced the transcription of Mdm2 after zinc induction. The p53 and Mdm2 levels were recorded using time-lapse fluorescent microscopy of the cell line clone expressing both fluorescent proteins after γ -irradiation at 20 minutes resolution during 16 hrs of growth (Figure 8). The results show that individual cells exhibit sustained oscillations in the p53-CFP and Mdm2-YFP nuclear levels in response to DSB's (Figure 8), but that the number of pulses varies from cell to cell. The width of each pulse was of 350 ± 160 min. The maximum of the first peak appeared 360 ± 240 min after DSB, and the time between successive peaks stabilized at a 440 ± 100 min. The time delay between the maximum levels of p53 and Mdm2 was ~ 100 min. However, some individual cells did not show pulses of p53 and Mdm2 after γ -irradiation.

The coincidence between the outputs from the models of Batchelor et al. (2008, 2011) and Ma et al., (2005) with their own and Lahav et al. (2004) experimental results, indicates that γ -irradiation produces DSB's that induces the onset of a limit cycle through a supercritical Hopf bifurcation in the p53-Mdm2 phase plane (Batchelor, 2008), and that the molecular mechanisms that underlay this dynamical behavior possibly lies on the p53-Mdm2 negative feedback loop (Figures 1a). However, the only existence of this loop seems not to be enough to explain the sustained oscillations observed in individual cells (Lahav et al., 2004; Ma et al., 2005; Batschelet et al., 2008, 2011).

According to the results from the model of Ma et al., (2005), the presence of DSB's induces a switch-like behaviour of the ATM kinase, which dissociates from its inactive dimmer form into two activated monomers that phosphorylate p53 (Figures 2a). This switch is turned on by doses of γ -irradiation as low as 0.1 Gy (~ 3 DSB's) and saturates at 0.4 Gy (~ 14 DSB's). Furthermore, activated ATM monomers (represented by ATM*) close a positive feedback loop acting on the ATM inactive dimmer form to cleavage it and produce more activated monomers. The combination of these two feedback loops is able of producing the sustained oscillations observed in individual cells.

However, experimental and theoretical analysis of the p53-Mdm2 loop by Batchelor et al. (2011) show that the sustained oscillations observed in individual cells can also be explained by the action of a triple negative feedback loop. ATM* activates p53, which closes the first negative feedback loop with Mdm2. However, p53 also activates the transcription of *wip1* that closes a negative feedback loop with p53. Although, p53 also closes a negative feedback loop with ATM* mediated by Wip1 (Figures 4). Experimental and *in silico* results (Batchelor et al., 2008, 2011) show that the suppression of the negative action of Wip1 on ATM* switches p53 dynamics from repetitive pulses into a single analog pulse.

Probably, the positive ATM feedback loop together with a initial rapid degradation of Mdm2 (Batchelor et al., 2011) and the triple negative feedback loops mediated by p53, Mdm2 and Wip1 accounts for the onset and stability of the limit cycle that gives rise to the digital response to γ -irradiation observed in individual cells.

Digital response of the p53 machinery to DSB by γ -irradiation could be a timing mechanism that controls downstream events that determine if the DSB's can be repaired or not (Figure 3a), and, in consequence, if apoptosis should continue until cell death or not (Ma et al., 2005; Dogu and Díaz, 2009).

4.2 Non-oscillatory nuclear dynamics of p53 in response to ionizing radiation

The effect of UV is the cross link of consecutive pyrimidine bases producing the exposition of single strands of DNA (ss-DNA). In contrast to the effect of γ -irradiation, the treatment of cells with bursts of UV-radiation with different energy, ranging from 2 to 10 J/m², produces, in each case, a single analog pulse whose amplitude and duration increases with the UV doses. (Batchelor et al., 2011).

Beside the difference in the type of damage produced by γ and UV irradiation to the DNA, digital and analog p53 dynamics are sustained by different feedback mechanisms. The presence of ss-DNA induces the activation of the ATR kinase, which phosphorylates Mdm2 on Ser-407, a rapid reversible process, and inhibits its activity on p53. In contrast, DSB's induces the activation of the ATM kinase, which phosphorylates Mdm2 on Ser-395, producing its rapid degradation and an initial sharp rise of p53 activity (Batchelor et al., 2011). In consequence, the initial inhibitory effect of ATR* on the p53-Mdm2 loop is less intense than the initial effect of ATM*. Furthermore, the restoration of this loop after the post-translational modification of Mdm2 by ATR* probably occurs in a time scale of minutes. In contrast, the restoration of the p53-Mdm2 loop after the rapid degradation of Mdm2 produced by ATM*, probably occurs in a time lapse of hours due to the process of translation of *mdm2*. Additionally, as Wip1 has not a detectable inhibitory action on ATR*, p53 has not a negative retroactivity on ATR* mediated by Wip1. In this form, there are only two persistent feedback loops acting on p53 after UV-irradiation: the p53-Mdm2 and the p53-Wip1. (Batchelor et al., 2008, 2011).

Additionally, in contrast to the switch-like activation of ATM in response to low doses of γ -irradiation, the rate of activation of ATR must be considered UV-doses dependent in order to computationally reproduce the analog dynamics of p53 (Batchelor et al., 2011). In this form, the analog response of p53 to UV-irradiation seems to be due to three facts: 1) rapid reversible inactivation of Mdm2 by ATR*; 2) absence of negative retroactivity of p53 on ATR* mediated by Wip1 and 3) a non switch-like dynamics of activation of ATR.

4.3 Heterogeneous oscillatory dynamics of p53 in cell populations

Previous experiments by Lahav et al. (2004) show that a population of cells from the same clone MCF7, exhibit damped oscillations of p53 and Mdm2, when their dynamics is recorded by assays based on the determination of the average or the relative values of the amount of proteins over populations of cells, like the immunoblot technique. When not such averaging techniques are used (see section 4.1), records of the dynamics of p53 and Mdm2 show sustained oscillations with wide heterogeneity in their amplitude, not only between isogenic cells, but also in individual cells (Figure 9).

Geva-Zatorsky et al. (2006) repeated the experiment mentioned in section 4.1, but with 30 h of continuous recording. They found that only 60% of the cells exposed to 10 Gy of γ -irradiation showed sustained oscillations of the p53-Mdm2 feedback loop. These oscillations have a relatively constant period of 5.5 ± 1.5 h, a high coefficient of variation (~ 0.7) in their amplitude, and a relatively constant peak width. The p53-Mdm2 delay is also relatively

constant in these cells. In contrast, only 30% of the cells exposed to 5 Gy of γ -irradiation showed sustained pulses, indicating that the number of cells displaying oscillations increases with higher doses of γ radiation. Initially, the onset of the oscillations in different cells was synchronized with the pulse of γ -radiation applied. However, synchrony was lost due to the different frequency response exhibited by individual cells. Some cells stopped their oscillatory dynamics or changed their frequency of oscillation. Additionally, after cell division, sister cells exhibited oscillations of p53 and Mdm2 that were initially synchronized. However, after a lapse of time of ~ 11 h this correlation decreased in 50%.

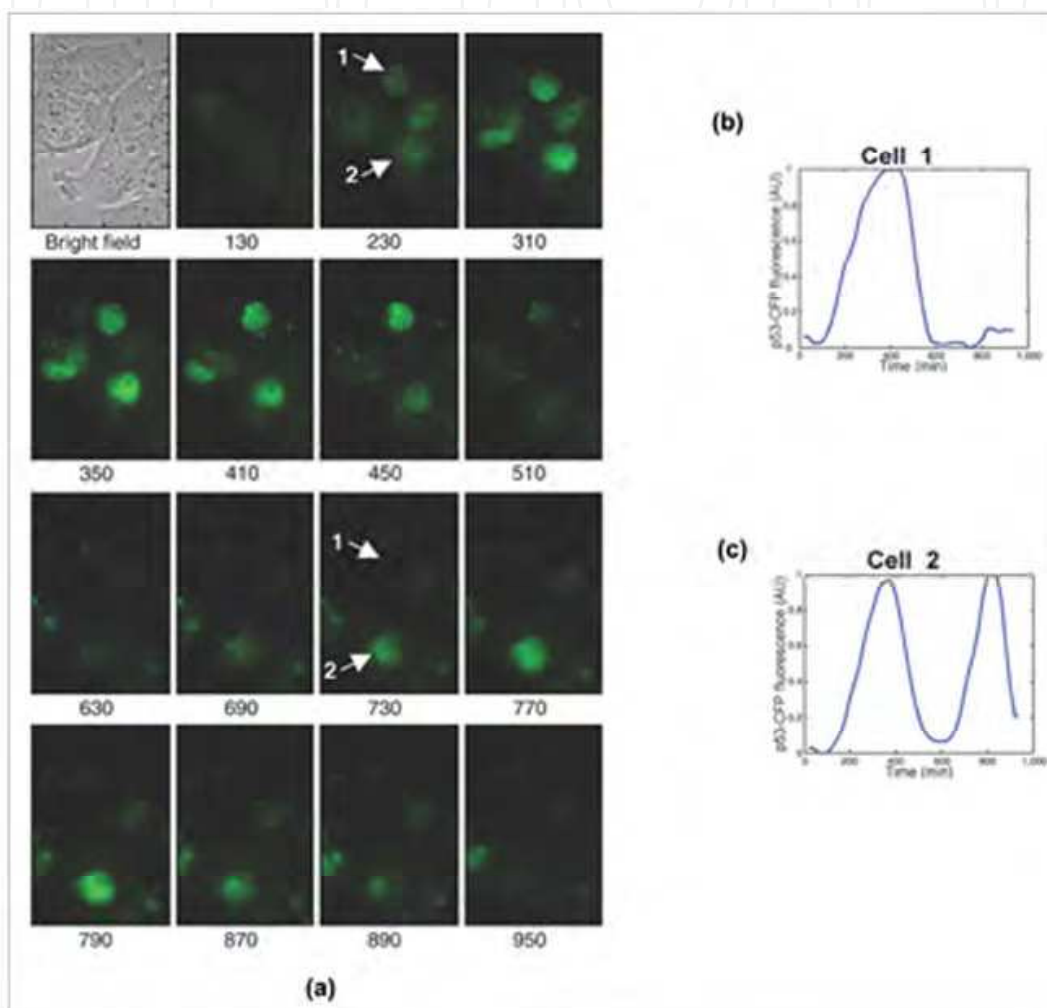


Fig. 9. (a) **p53-CFP (green)** in clonal MCF7+pU265+pU293 cells after 5-Gy γ -irradiation. Time (in min) after irradiation is shown below images. (b) and (c) **p53-CFP levels** (total CFP fluorescence in nuclei) from cells 1 and 2 (indicated by arrows in (a)), showing the heterogeneity in the pulses generated after γ -irradiation. AU, arbitrary units. Figure reproduced from Lahav et al. (2004), with authorization of Dr. U. Alon.

Geva-Zatorsky et al. (2006) work also reveals that after a treatment with 10Gy of γ -radiation, 40% of the cells showed a non-oscillatory response, or did not respond at all. The non-oscillatory response consisted of slow fluctuations of Mdm2-YFP and p53-CFP with only one, two or three peaks. Each fluctuation had duration of 8 - 12 h. Furthermore, a fraction of non-irradiated cells also show this kind of fluctuations.

4.4 Noisy oscillatory dynamics of p53

From section 4.3, it is clear that a deterministic approach for understanding the dynamics of apoptosis is not enough to account for the heterogeneity observed in the p53-Mdm2 oscillatory response of individual cells to IR. As we mentioned in section 3.3, the onset of a stable limit cycle in the p53-Mdm2 phase plane depends on the transition from a stable spiral to an unstable spiral (supercritical Hopf bifurcation), according to the Poincaré-Bendixson and Hopf theorems. Once the limit cycle is settled down, all nearby trajectories are trapped by it. In this form, any small perturbation of this cycle will be damped and the system will return slowly to its original rhythm of oscillation with constant amplitude and frequency. This is not the kind of dynamical behavior experimentally determined in MCF7 cells (Ma et al., 2005; Batchelor et al., 2011; Lahav et al., 2004; Geva-Zatorski et al., 2006). As consequence, deterministic models of the p53-Mdm2 oscillations can be considered only as approximate descriptions of reality if they take into account only the p53-Mdm2 negative feedback loop (Qi et al., 2007; Spencer and Sorger, 2011). As it was mentioned in section 4.1, better results are obtained from models that take into account the positive ATM feedback loop together with a initial rapid degradation of Mdm2 (Ma et al., 2005; Batchelor et al., 2011; Jolma et al., 2010) and the triple negative feedback loops mediated by p53, Mdm2 and Wip1. From these models, it is clear that in the nuclear compartment the activation of the dynamical characteristics of the DNA repairing molecular machinery conveys a trajectory that sharply leads to an unstable fixed point in the ATM*-p53-Mdm2 phase space, from which a limit cycle parallel to the p53-Mdm2 plane emerges through a supercritical Hopf bifurcation. However, there is also the possibility of the existence of a subcritical Hopf bifurcation, which can then lead to cycles of different IR-dose dependent amplitude (Qi et al., 2007). Nevertheless, these models cannot account for the variability of the pulses of p53 and Mdm2 observed in individual cells and in cell populations.

Cell systems are subject to intrinsic and extrinsic noise sources that can affect both the rate of production and the rate of degradation of proteins (Elowitz et al., 2002; Kaufmann and van Oudenaarden, 2006). Noise is a source of variability, even in cells from the same cell line. The intrinsic cell noise can insert a low frequency fluctuating component in the rate of production (degradation) of proteins producing a continuous stochastic variation in the corresponding number of molecules (Diaz, 2011). Geva-Zatorski et al. (2006) point out that the probable source of variability in the response of cells to γ -radiation is the stochastic variation in the rate of protein production, which generates fluctuations in the amplitude of the pulses without affecting their period. On the contrary, if the protein degradation rate is affected by noise, pulses exhibit variable amplitude and period. In this form, fluctuations in the rate of the transcription and translation processes of key apoptotic proteins after DSB damage can be reflected in the variable amplitude of the p53 and Mdm2 pulses, without affecting their rhythm of generation.

Furthermore, fluctuations can evoke the generation of spontaneous elevations in the basal concentrations of Mdm2, even in absence of γ -irradiation (Geva-Zatorski et al., 2006). Cancer cells have a unstable genetic system in which is possible that some control mechanism of apoptosis are modified or disabled in order to undergo cell death in response to cytotoxic stimuli. In consequence, any spontaneous fluctuations in the concentration of apoptotic nuclear proteins, like Mdm2, can be over amplified giving rise to the atypical dynamical features of cancer cells. For example, spontaneous increase in the concentration of Mdm2 can suppress the activity of p53 by ubiquitination and posterior degradation in the proteasome (Figure 1a), and disable the apoptotic mechanism of MCF7 cells during time lapses up to ~ 20 h (Geva-Zatorski et al., 2006).

After MCF7 cells division, p53 and Mdm2 oscillations continued with the same phase but sister cells lose $\sim 50\%$ of correlation in their oscillatory dynamics after 11 h (Geva-Zatorski et al., 2006). These results point to two important facts: 1) apoptotic information can be transferred to daughter cells and 2) sister cells can inherit similar levels of relevant apoptotic molecules, but noise generates fluctuations in protein production and degradation. As consequence, synchrony is lost after a lapse of time (Spencer and Sorger, 2011). In this form, the initial apoptotic timing synchronization caused by the γ -irradiation can be transferred to daughter cells but this correlation falls as time from division increases, until sister cells are no more correlated than a randomly chosen pair of cells (Spencer and Sorger, 2011).

4.5 Dynamics of cytoplasmic apoptotic proteins

Bistability is a broad dynamical feature of nonlinear biochemical systems, in which an unstable steady point separates two stable nodes. The transition between nodes requires energy to overcome the high energetic barrier among them. Generally, once the transition from one steady point to the other occurs, return to the original state requires a different pathway with different energy requirements, forming a **hysteresis** loop. Molecular switches are the common examples of this type of dynamics (Strogatz, 1994).

Bagci et al. (2006) work studied the role of Bax and Bcl2 synthesis and degradation rates in mitochondria-dependent apoptosis (Figure 3a), finding the existence of a saddle point bifurcation in the caspase 3-Bax degradation rate diagram. The Bax degradation rate of $\sim 0.11 \text{ s}^{-1}$ determines the upper limit to this region of bistability. Inside this region, the saddle point bifurcation can drive the system either to a stable point with a high concentration of caspase 3 (cell death) or to a stable point with a low concentration of caspase 3 (cell survival). Out of this region, the systems dynamics is settled on by the existence of a single stable fix point that determines cell surviving independently of the concentration of caspase 3. Cui et al. (2008) work points out that the activation of the "Bcl2 switch" upstream mitochondria induces apoptosis when the formation of the heterodimer Bak/Bax reaches a certain level. In this form, Bax level settles on the beginning of the apoptosis process (Bagci et al., 2006; Cui et al., 2008; Hua et al., 2005). An important conclusion from this work is that an abnormal state, like cancer, arises in cells when Bax degradation rate is above a threshold value, giving rise to a stable cell survival dynamics, i.e., cells do not die.

Fussenegger, Bailey and Varner (2000) work used mass-conservation law and kinetic rate laws to establish a model of caspases 8 and 9 activation by the extrinsic and intrinsic apoptotic pathways respectively. According to this model, in the case of the intrinsic pathway the release of cytochrome c starts 10 min after a stress signal like IR. The executioner caspases are active at 40% of its maximum value 1 h after the initiation of the stress response and 70% of them are active 2 h after. A negative mutation in p53 decreases the fraction of both activated caspase 9 and executioner caspases.

Dogu and Díaz (2009) model takes into account the role of proapoptotic proteins like p53 and Puma in the response to stress signals like IR (Figure 3a). This model shows that the overall kinetic behaviour of the p53 apoptotic network under genotoxic stress is mainly due to a possible p53-induced release of Bax from its complex with Bcl2 even in absence of Puma. However, the release of Puma in the cytoplasm increases the rate of liberation of Bax from the Bcl2/Bax cytoplasmic complex. In this form, this model proposes that Bax cytoplasmic level controls apoptosis by its continuous release from the Bcl2/Bax complex after DNA damage. If DNA is repaired or the damage is reduced enough before Bax reaches a threshold value, cells may divide or may have a Bax control mechanism that avoids the

start of apoptosis. In this model PUMA plays the role of accelerator of the Bax level increasing process. The possible biological significance of this process may be to allow a lag between the starting of the DNA damage repair process and the onset of full apoptosis when the damage cannot be repaired in a pre-set moment of the cell cycle. After this time lag, Puma reaches a threshold concentration value that fires the complete and irreversible apoptotic process. From a dynamical point of view, this model states the stability and robustness of the network of interaction between p53 and the pro and anti-apoptotic proteins BclxL, Bcl2, Puma and Bax. The flow predicted by this model is formed by set of trajectories that converge into an attractor in the 4-dimensional phase space spanned by the concentration of the p53/Bcl-x_L, PUMA/Bcl-x_L, Bax/Bcl2 and p53/Bcl2 complexes. This flow is reasonably independent of the values of the rate constants of association and dissociation of these complexes, indicating its structural stability.

In this form, the cytoplasmic component of the apoptotic subnetwork exhibits a dynamics driven by a saddle-node bifurcation, which settles down a control point that determine the cell fate according to the information flow from the nucleus. This dynamics seems to be started by a Bcl2 switch that initiates the accumulation of Bax in the cytoplasm, until it reaches a threshold value. It seems that, although the cytoplasmic accumulation of Bax initiates the liberation of cytochrome c from mitochondria in a time lapse as short as ~ 10 min, the process is still reversible. However, once PUMA is present in the cytoplasm, the rate of liberation of Bax from the Bcl2/Bax complexes is sharply increased, and makes the apoptotic process completely irreversible due to the consequent increase of the levels of Bax over its threshold value. The high concentration of free Bax triggers the process of activation of caspase 3.

5. Conclusions

Apoptosis is a complex molecular process, which is capable of determine the cell fate according to the intensity of the DNA damage caused by IR (section 2.3). This network of molecular processes has a highly connected node, which is protein p53. Its key role in apoptosis is tightly regulated by a series of molecules like Wip1 and Mdm2, among others. DSB's and ss-DNA can trigger the activation of either ATM or ATR (section 2.4). These kinases suppress the inhibitory activity of Mdm2 on p53, giving rise to a digital or to an analog response to IR, respectively (section 4.1 and 4.2).

Cancer cells show abnormalities in their genetic network, which includes the regulatory loops of apoptosis. As a result, the cancer cell response to IR is heterogeneous probably due to three facts: 1) IR produces random damage to DNA (Ma et al., 2005; Qi et al., 2007); 2) intrinsic noise adds some amount of randomness to the processes of transcription and translation of key apoptotic proteins (Geva-Zatorsky et al., 2006; Díaz, 2011); 3) regulatory genetic loops may be randomly disabled in cancer cells.

The effect of randomness is the generation of low frequency fluctuations in the levels of proteins like Mdm2. When these fluctuations coincide with the natural frequency of oscillation of the negative feedback loops that control p53 activation, the result is a series of pulses of different amplitude (Geva-Zatorsky et al., 2006). However, the rhythm of the oscillations remains relatively constant, suggesting that fluctuations principally affect the rate of synthesis of proteins. Models that include this randomness are successful in reproducing the heterogeneity of the pulses of p53 and Mdm2 in individual cells (Section 4.3).

However, there are not data about the oscillatory dynamics of p53 in normal cells after perturbation with IR, neither in other lines of cancer cells. In this form, it is not known if the

oscillatory dynamics found in MCF7 cells represents a generalized dynamical behaviour of all cells under treatment with IR, or if it is only a particular feature of this cell line. However, variability in response to other proapoptotic treatments seems to be an universal feature of cells (Spencer and Sorger, 2011). A direct and very important consequence of this variability is that the killing fraction, i.e., the fraction of died cells from an initial living cell population after treatment with a proapoptotic agent, is generally much lower than 100%. This fact points to the necessity of combining at least two different treatments to completely eradicate cancer cells.

In order to gain a deeper insight into the mechanisms that generate this variability in cell response, is necessary to elaborate a more rigorous quantitative approach to understand how key apoptotic processes are affected by stochasticity. Mathematical and computational models, combined with quantitative experimental research, are necessary tools to achieve this goal.

As we stated in this chapter, deterministic models of apoptosis seems to have a limited power to explain the real dynamics of cell death. However, they are still useful tools because they incorporate in their core of equations a series of kinetic terms that represent the contribution of the different biochemical process at different times. Furthermore, from these models some general principles about the dynamics of apoptosis are beginning to emerge: 1) digital and analog responses are generated by different mechanisms of activation and regulation of p53; 2) digital response is generated by the nonlinear interaction of at least three negative feedback loops and an autocatalytic process, together with the rapid initial degradation of Mdm2 that generates a time delay in the restoration of its negative feedback loop with p53; 3) this nonlinear interactions conveys the evolution of the dynamical system to an unstable fixed point in the ATM*-p53-Mdm2 phase space, from which a limit cycle parallel to the p53-Mdm2 plane emerges through a supercritical Hopf bifurcation; 4) this limit cycle assures the stability of the oscillations, generating pulses of constant peak width, frequency and average amplitude; 5) as consequence, deterministic models predicts the onset of a clock-like mechanisms that determines the timing of cell death; 6) this nuclear clock may be somehow synchronized with the cytoplasmic events that lead to the activation of executory caspases; 7) cytoplasmic biochemical processes generated by the interaction of pro-apoptotic and anti-apoptotic molecules like p53, PUMA, Bcl2, Bak, Bax, among others, settle down a saddle-node bifurcation, which determines either cell death or cell survival, depending on the levels of free Bax; 8) with respect to the nuclear analog response, deterministic models suggest that is due to the activation of only two negative feedback loops and the rapid reversible modification of Mdm2 by ATR*.

However, it is necessary to propose a broader deterministic model in order to understand: 1) how the nuclear Hopf bifurcation is linked to the cytoplasmic saddle-node bifurcation to determine the precise timing of cell death and 2) how the correct death-survival decision is taken according to the information processed in the nucleus.

Stochasticity can be added to this model in order to know if the fluctuations of p53 in the nucleus also influence death decisions in the cytoplasm, or if they are damped by the cytoplasmic feedback loops, avoiding lose of the correct timing of apoptosis. Mislay of this timing can produce cell death at random lapses of time.

Finally, the knowledge generated by stochastic models can be useful to improve the proapoptotic treatments that are used now day. These treatments can target nodes that are not practically affected by noise, allowing the increase of the killing fraction.

6. Acknowledgments

We thank Erika Juarez Luna for technical and logistical assistance. Financial support for this work was from CONACYT (Consejo Nacional de Ciencia y Tecnología) grant 105678.

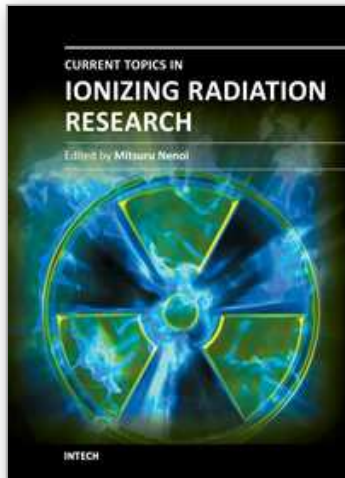
7. References

- Abukhdeir AM & Park BH (2008). p21 and p27: roles in carcinogenesis and drug resistance. *Expert Rev Mol Med*. 10:e19; doi: 10.1017/S1462399408000744.
- Andronov AA, Leontovich EA, Gordon II, & Maier AG (1973). *Qualitative theory of second order dynamic systems*. J. Wiley. New York, NY. ISBN: 0470031956
- Bagci EZ, Vodovotz Y, Billiar TR, Ermentrout GB & Bahar I (2006). Bistability in apoptosis: roles of Bax, Bcl-2, and mitochondrial permeability transition pores. *Biophysical Journal* 90:1546–1559.
- Baillat D, Laitem C, Leprivier G, Margerin C & Aumercier C (2008). Ets-1 binds cooperatively to the palindromic Ets-binding sites in the p53 promoter. *Biochemical and Biophysical Research Communications* 378: 213–217.
- Batchelor E, Loewer A, Mock C & Lahav G (2011). Stimulus-dependent dynamics of p53 in single cells. *Molecular Systems Biology* 7:488; doi:10.1038/msb.2011.20
- Batchelor E, Mock CS, Bhan I, Loewer A & Lahav G (2008). Recurrent Initiation: A Mechanism for Triggering p53 Pulses in Response to DNA Damage. *Molecular Cell* 30: 277–289.
- Bergamaschi D, Samuels Y, Jin B, Duraisingham S, Crook T & Lu X (2004). ASPP1 and ASPP2: Common Activators of p53 Family Members. *Molecular and Cellular Biology* 24: 1341-1350.
- Bernards R (2004). Wip-ing out cancer. *Nature Genetics* 36: 319-320.
- Boogs K & Reisman D (2007). C/EPB β Participates in Regulating Transcription of the p53 Gene in Response to Mitogen Stimulation. *The Journal of Biological Chemistry* 282: 7982–7990.
- Braithwaite AW (2006). Some p53-binding proteins that can function as arbiters of life and death. *Cell Death and Differentiation* 13: 984–993.
- Budirahardja Y & Gönczy P (2009). Coupling the cell cycle to development. *Development* 136:2861-2872.
- Calonge TM & O'Connell MJ (2008). Turning off the G2 DNA damage checkpoint. *DNA Repair* 7:136–140.
- Candeias MM, Malbert-Colas L, Powell DJ, Daskalogianni C, Maslon MM, Naski N, Bourougaa K, Calvo F & Fähræus R (2008). p53 mRNA controls p53 activity by managing Mdm2 functions. *Nature Cell Biology* 19: 1098-1105.
- Chen C, Edelstein LC & Gélinas C (2000). The Rel/NF- κ B Family Directly Activates Expression of the Apoptosis Inhibitor Bcl-xL. *Molecular and Cellular Biology* 20:2687–2695.
- Cui J, Chen C, Lu H, Sun T, Shen P (2008). Two independent positive feedbacks and bistability in the Bcl-2 apoptotic switch. *Plos One* 3: e1469; doi:10.1371/journal.pone.0001469.
- Daniel P, Teufel, Stefan M, Freund, Mark Bycroft, and Alan R. Fersht 2007 Four domains of p300 each bind tightly to a sequence spanning both transactivation subdomains of p53. *PNAS*, 104: 7009–7014.
- Del Vecchio D, Ninfa AJ & Sontag ED (2008). Modular cell biology: retroactivity and insulation. *Molecular Systems Biology* 4:161; doi:10.1038/msb4100204

- Díaz J (2011). Information flow in plant signaling pathways. *Plant Signaling & Behavior* 2011 6: 1-5.
- Dogu Y & Díaz J (2009). Mathematical model of a network of interaction between p53 and Bcl-2 during genotoxic-induced apoptosis. *Biophysical Chemistry* 143:44-54.
- Edelstein-Keshner L (2005). *Mathematical Models in Biology. Classics in Applied Mathematics.* Siam. Philadelphia, PA. ISBN: 978-0-898715-54-5.
- Elowitz MB, Levine AJ, Siggia ED, Swain PS (2002). Stochastic Gene Expression in a Single Cell. *Science* 297: 1183-86.
- Fussenegger M, Bailey JE, Varner J (2000) A mathematical model of caspase function in apoptosis. *Nature Biotechnology* 18:768-774.
- Geva-Zatorsky N, Rosenfeld N, Itzkovitz S, Milo R, Sigal A, Dekel E, Yarnitzky T, Liron Y, Polak P, Lahav G & Alon U (2006). Oscillations and variability in the p53 system. *Molecular Systems Biology* 2:2006.0033; doi:10.1038/msb4100068.
- Green DR & Kroemer G (2009). Cytoplasmic functions of the tumour suppressor p53. *Nature* 458: 1127-1130.
- Haupt S, Alsheich-Bartok O and Haupt Y (2006) Clues from worms: a Slug at Puma promotes the survival of blood progenitors. *Cell Death and Differentiation* 13:913-915.
- Hu W, Feng Z, Ma L, Wagner J, Rice JJ, Stolovitzky G & Levine AJ (2007). A Single Nucleotide Polymorphism in the MDM2 Gene Disrupts the Oscillation of p53 and MDM2 Levels in Cells. *Cancer Research* 67: 2757-2765.
- Hua F, Cornejo MG, Cardone MH, Stokes CL & Lauffenburger DA (2005). Effects of Bcl2 Levels on Fas signaling-induced caspase-3 activation: molecular genetic tests of computational model predictions. *The Journal of Immunology* 175:985-995.
- Ikenoue T, Inoki K, Zhao B & Guan K (2008). PTEN Acetylation Modulates Its Interaction with PDZ Domain. *Cancer Research* 68: 6908-6912.
- Jänicke RU, Sohn D & Schulze-Osthoff K (2008). The dark side of a tumor suppressor: anti-apoptotic p53. *Cell Death and Differentiation* 15: 959-976.
- Jolma IW, Ni XY, Rensing L, & Ruoff P (2010). Harmonic Oscillations in Homeostatic Controllers: Dynamics of the p53 Regulatory System. *Biophysical Journal* 98: 743-752.
- Kaufmann BB & van Oudenaarden A (2007). Stochastic gene expression: from single molecules to the proteome. *Current Opinion in Genetics & Development* 17:107-12.
- Kobet E, Zeng X, Zhu Y, Keller D & Lu H (2000). MDM2 inhibits p300-mediated p53 acetylation and activation by forming a ternary complex with the two proteins. *PNAS* 97:12547-12552.
- Lacroix M, Toillon R & Leclercq G (2006). p53 and breast cancer, an update. *Endocrine-Related Cancer* 13: 293-325.
- Lahav G, Rosenfeld N, Sigal A, Geva-Zatorsky N, Levine AJ, Elowitz MB & Alon U (2004). Dynamics of the p53-Mdm2 feedback loop in individual cells. *Nature Genetics* 36:147-150.
- Liu Z, Lu H, Shi H, Du Y, Yu J, Gu S, Chen X, Liu KJ & Hu CA (2005). PUMA Overexpression Induces Reactive Oxygen Species Generation and Proteasome-Mediated Stathmin Degradation in Colorectal Cancer Cells. *Cancer Res.* 65:1647-1654.
- Lu X, Nguyen T, Moon S, Darlington Y, Sommer M & Donehower LA (2008). The type 2C phosphatase Wip1: An oncogenic regulator of tumor suppressor and DNA damage response pathways. *Cancer Metastasis Rev.* 27:123-135

- Ma L, Wagner J, Rice JJ, Hu W, Levine AJ & Stolovitzky GA (2005). A plausible model for the digital response of p53 to DNA damage. *PNAS* 102: 14266–14271.
- Malumbres, M & Barbacid M (2009). Cell cycle, CDKs and cancer: a changing paradigm. *Nature Reviews Cancer* 3:153-166.
- Marquez RT, Baggerly KA, Patterson AP, Liu J, Broaddus R, Frumovitz M, Atkinson EN, Smith DI, Hartmann L, Fishman D, Berchuck A, Whitaker R, Gershenson DM, Mills GB, Bast RC & Lu KH (2004). Selection of Potential Markers for Epithelial Ovarian Cancer with Gene Expression Arrays and Recursive Descent Partition Analysis. *Clinical Cancer Research* 11: 3291–3300.
- Méndez O, Martín B, Sanz R, Aragüés R, Moreno V, Oliva B, Stresing V & Sierra A (2006) Underexpression of transcriptional regulators is common in metastatic breast cancer cells overexpressing Bcl-xL. *Carcinogenesis*, 27:1169–1179.
- Michael Karin & Anning Lin (2002). NF- κ B at the crossroads of life and death. *Nature Immunology* 3: 221-227.
- Patel S, George R, Autore F, Fraternali F, Ladbury JE & Nikolova PV (2008). Molecular interactions of ASPP1 and ASPP2 with the p53 protein family and the apoptotic promoters PUMA and Bax. *Nucleic Acids Research* 36: 5139–5151.
- Pediconi N, Guerrieri F, Vossio S, Bruno T, Belloni L, Valeria Schinzari V, Scisciani C, Fanciulli M & Levrero M (2009). hSirT1-Dependent Regulation of the PCAF-E2F1-p73 Apoptotic Pathway in Response to DNA Damage. *Molecular and Cellular Biology* 29:1989–1998.
- Perry ME (2004). Mdm2 in the Response to Radiation. *Molecular Cancer Research*, 2: 9-19.
- Phelps M, Darley M, Primrose JN & Blaydes JP (2003). p53-independent Activation of the hdm2-P2 Promoter through Multiple Transcription Factor Response Elements Results in Elevated hdm2 Expression in Estrogen Receptor α -positive Breast Cancer Cells. *Cancer Research* 63: 2616–2623.
- Pietsch EC, Sykes SM, McMahon SB & Murphy ME (2008). The p53 family and programmed cell death. *Oncogene* 27:6507–6521.
- Plati J, Bucur O & Khosravi-Far R (2011). Apoptotic cell signaling in cancer progression and therapy. *Integrative Biology* 3: 279–296
- Pommier Y & Weinstein JN (2006). Chk2 Molecular Interaction Map and Rationale for Chk2 Inhibitors. *Clin Cancer Res.* 12: 2657–2661.
- Qi JP, Shao SH, Xie J & Zhu Y (2007). A mathematical model of P53 gene regulatory network under radiotherapy. *BioSystems* 90: 698–706
- Robinson RA, Lu X & Edith Yvonne Jones EY (2008). Biochemical and Structural Studies of ASPP Proteins Reveal Differential Binding to p53, p63, and p73. *Structure* 16 : 259–268.
- Schmid JA & Birbach A (2008). I κ B kinase β (IKK β /IKK2/IKBKB)—A key molecule in signaling to the transcription factor NF- κ B. *Cytokine & Growth Factor Reviews* 19:157–165.
- Shreeram S, Demidov ON, Hee WK, Yamaguchi H, Onishi N, Kek C, Timofeev ON, Dudgeon C, Fornace AJ, Anderson CW, Minami Y, Appella E & Bulavin DV (2006). Wip1 Phosphatase Modulates ATM-Dependent Signaling Pathways. *Molecular Cell* 23: 757–764.
- Spencer LS & Sorger PK (2011). Measuring and Modeling Apoptosis in Single Cells. *Cell* 144:926-939.
- Stewart RD (2001). Two-Lesion Kinetic Model of Double-Strand Break Rejoining and Cell Killing. *Radiation Research* 156: 365–378.

- Strano S, Dell'Orso S, Mongiovi AM, Monti O, Lapi E, Di Agostino S, Fontemaggi G & Blandino G (2006). Mutant p53 proteins: between loss and gain of function. *Head and Neck* 29: 488-496.
- Strogatz S (1994). *Nonlinear Dynamics and Chaos. With applications to Physics, Biology, Chemistry, and Engineering*. Perseus Books Publishing, LLC. Cambridge, MA. ISBN: 978-0-7382-0453-6.
- Sun Y, Jiang X, Chen S, Fernandes N & Price BD (2005). A role for the Tip60 histone acetyltransferase in the acetylation and activation of ATM. *PNAS* 102: 13182-13187.
- Tanaka T, Huang X, Halicka HD, Zhao H, Traganos F, Albino AP, Dai W, Darzynkiewicz Z (2007). Cytometry of ATM Activation and Histone H2AX Phosphorylation to Estimate Extent of DNA Damage Induced by Exogenous Agents. *Journal of the International Society for Analytical Cytology* 71A: 648-661.
- Tanno M, Sakamoto J, Miura T, Shimamoto K & Horio Y (2006). Nucleo-cytoplasmic shuttling of NAD⁺-dependent histone deacetylase SIRT1. *The Journal of Biological Chemistry*, 282: 6823-6832.
- Thieffry D & Romero D (1999). The modularity of biological regulatory networks. *Biosystems* 50:49-59.
- Toledo F & Wahl GM (2006). Regulating the p53 pathway: in vitro hypotheses, in vivo veritas. *Nature Reviews Cancer* 6: 909-923.
- Vissers JHA, Nicassio F, van Lohuizen M, Di Fiore P, Citterio E (2008). The many faces of ubiquitinated histone H2A: insights from the DUBs. *Cell Division* 3:8; doi:10.1186/1747-1028-3-8
- Vousden, Karen H (2006). Outcomes of p53 activation - spoilt for choice. *Journal of Cell Science* 119: 5015-5020.
- Wagner J, Ma L, Rice JJ, Hu W, Levine AJ & Stolovitzky G (2005). p53-Mdm2 loop controlled by a balance of its feedback strength and effective dampening using ATM and delayed feedback. *IEE Proc.-Syst. Biol.* 152:109-118.
- Wang P, Yu J & Zhang L (2007). The nuclear function of p53 is required for PUMA-mediated apoptosis induced by DNA damage. *PNAS* 104:4054-4059.
- Wang S & El-Deiry WS (2006) p73 or p53 Directly Regulates Human p53 Transcription to Maintain Cell Cycle Checkpoints. *Cancer Research* 66: 6982-6989 .
- Wu H & Lozano G (1994). NF- κ B Activation of p53 A POTENTIAL MECHANISM FOR SUPPRESSING CELL GROWTH IN RESPONSE TO STRES. *The Journal of Biological Chemistry*, 269:20067-20074.
- Yamamori T, DeRico J, Naqvi A, Hoffman TA, Mattagajasingh I, Kasuno K, Jung S, Kim C & Irani K (2009) SIRT1 deacetylates APE1 and regulates cellular base excision repair. *Nucleic Acids Research* 38: 832-845.
- Yoda A, Toyoshima K, Watanabe YY, Onishi N, Hazaka Y, Tsukuda Y, Tsukada J, Kondo T, Tanaka Y & Minami Y (2008). Arsenic Trioxide Augments Chk2/p53-mediated Apoptosis by Inhibiting Oncogenic Wip1 Phosphatase. *The Journal of Biological Chemistry* 283: 18969-18979.
- Youle RJ & Strasser A (2008). The BCL-2 protein family: opposing activities that mediate cell death. *Nature Reviews in Molecular Cell Biology* 9:47-59.
- Zhang J, Tsapralis G & Bowden GT (2008) Nucleolin Stabilizes Bcl-XL Messenger RNA in Response to UVA Irradiation. *Cancer Research* 68: 1046-1054.
- Zhang X, Feng Liu F, Cheng Z & Wang W (2009). Cell fate decision mediated by p53 pulses. *PNAS* 106: 12245-12250.



Current Topics in Ionizing Radiation Research

Edited by Dr. Mitsuru Neno

ISBN 978-953-51-0196-3

Hard cover, 840 pages

Publisher InTech

Published online 12, February, 2012

Published in print edition February, 2012

Since the discovery of X rays by Roentgen in 1895, the ionizing radiation has been extensively utilized in a variety of medical and industrial applications. However people have shortly recognized its harmful aspects through inadvertent uses. Subsequently people experienced nuclear power plant accidents in Chernobyl and Fukushima, which taught us that the risk of ionizing radiation is closely and seriously involved in the modern society. In this circumstance, it becomes increasingly important that more scientists, engineers and students get familiar with ionizing radiation research regardless of the research field they are working. Based on this idea, the book "Current Topics in Ionizing Radiation Research" was designed to overview the recent achievements in ionizing radiation research including biological effects, medical uses and principles of radiation measurement.

How to reference

In order to correctly reference this scholarly work, feel free to copy and paste the following:

Antonio Bensussen and José Díaz (2012). Dynamical Aspects of Apoptosis, Current Topics in Ionizing Radiation Research, Dr. Mitsuru Neno (Ed.), ISBN: 978-953-51-0196-3, InTech, Available from: <http://www.intechopen.com/books/current-topics-in-ionizing-radiation-research/dynamical-aspects-of-apoptosis>

INTECH
open science | open minds

InTech Europe

University Campus STeP Ri
Slavka Krautzeka 83/A
51000 Rijeka, Croatia
Phone: +385 (51) 770 447
Fax: +385 (51) 686 166
www.intechopen.com

InTech China

Unit 405, Office Block, Hotel Equatorial Shanghai
No.65, Yan An Road (West), Shanghai, 200040, China
中国上海市延安西路65号上海国际贵都大饭店办公楼405单元
Phone: +86-21-62489820
Fax: +86-21-62489821

© 2012 The Author(s). Licensee IntechOpen. This is an open access article distributed under the terms of the [Creative Commons Attribution 3.0 License](#), which permits unrestricted use, distribution, and reproduction in any medium, provided the original work is properly cited.

IntechOpen

IntechOpen